ALFVEN WAVE INSTABILITY BASED ON TEMPERATURE ANISOTROPY WITH NON-MAXWELLIAN DISTRIBUTION FUNCTION

M.N.S. Qureshi, Sundas Saeed, H.A. Shah

Department of Physics, GC University, Lahore 54000, Pakistan

Space observations by numerous satellites reveal that the distributions often possess non-Maxwellian characteristics such as high energy tails or flat top (broad shoulders) in the profile of distribution functions. Distributions with high energy tails are well modelled by family of kappa type distribution. However, when distributions contain flat tops with or without high energy particles, generalized (*r*,*q*) distribution function is the best choice. In general the spectral index *r* corresponds to the flat part of the distribution and *q* to the high energy tail in the profile of the distribution function. By following the kinetic theory, we employ this distribution function to study the Alfven waves in anisotropic plasma and found that Alfven wave can grow when there is temperature anisotropy in plasma. Instability conditions are then studied for different temperature ratios by using the plasma parameters observed downstream the bow shock by CLUSTER.

PACS: 52.27Aj; 52.35Hr; 52.35Qz

INTRODUCTION

Both in astrophysical and space plasmas Alfven waves are found to play major role in the dynamics of many planetary processes like in the dynamics of Earth's magnetosphere such as in the plasmasphere[1], in central plasma sheet [2], in tail lobes [3], in plasma sheet boundary layer (PSBL) [4-6], in magnetotail lobe region [7], in magnetotail reconnection region [8], and in solar corona [9]. In the solar wind Alfven waves accelerate the charged particles like protons, electrons and helium by transferring its energy to these particles through resonant interactions. Being feasible source of parallel electric fields Alfven waves are also believed to accelerate the electrons in auroral region which further generates fascinating auroras [8, 9]. Investigating the heating mechanism of solar atmosphere through Alfven waves, efforts are made to produce controlled fusion reactions in laboratory plasmas.

Alexandrova et al. [10] observed Alfven waves downstream of a quasi-perpendicular shock by Cluster and showed that anisotropies in the proton and alpha particles temperature can destabilize the Alfven waves. Similar observations have also been reported by Anderson et al. [11] and Gary et al. [12]. In this paper, we employed a non-Maxwellian distribution such as generalized (*r*,*q*) distribution function and study the instability criteria for Alfven waves based on the temperature anisotropy observed downstream of the Earth's bow shock.

1. DISTRIBUTION FUNCTION AND DISPERSION RELATION

The generalized (*r*,*q*) distribution function has the form:

$$f_{(r,q)} = \frac{3\,(q-1)^{-\frac{3}{2\,(r+1)}}\,\Gamma[q]}{4\,\pi\,\psi_\perp^2\psi_\parallel\,\Gamma\left[q-\frac{3}{2\,(r+1)}\right]\Gamma\left[1+\frac{3}{2\,(r+1)}\right]}\times \times\left[1+\frac{1}{(q-1)}\left\{\left(\frac{v_\parallel}{\psi_\parallel}\right)^2+\left(\frac{v_\perp}{\psi_\perp}\right)^2\right\}^{r+1}\right]^{q-1} \quad (1)$$

Here, $\psi_\parallel$ and $\psi_\perp$ are the modified thermal velocities of particles, given as

$$\psi_\parallel = \sqrt{\frac{T_\parallel}{m}}\sqrt{\frac{3\,(q-1)^{-\frac{1}{1+r}}\Gamma\left[q-\frac{3}{2\,(r+1)}\right]\Gamma\left[\frac{3}{2\,(r+1)}\right]}{\Gamma\left[q-\frac{5}{2\,(r+1)}\right]\Gamma\left[\frac{5}{2\,(r+1)}\right]}} \quad (2)$$

$$\psi_\perp = \sqrt{\frac{T_\perp}{m}}\sqrt{\frac{3\,(q-1)^{-\frac{1}{1+r}}\Gamma\left[q-\frac{3}{2\,(r+1)}\right]\Gamma\left[\frac{3}{2\,(r+1)}\right]}{\Gamma\left[q-\frac{5}{2\,(r+1)}\right]\Gamma\left[\frac{5}{2\,(r+1)}\right]}} \quad (3)$$

Where $T_\parallel$ and $T_\perp$ are parallel and perpendicular temperatures, Γ is the usual Gamma function, *m* is the mass of the particle, r and q are the spectral indices satisfying the conditions $q>1$ and $q(1+r)>5/2$. The distribution $f_{(r,q)}$ is the generalization of Maxwellian and Lorentzian distributions and in the limiting cases when $r=0$ and $q\to\kappa+1$, $f_{(r,q)}$ reduces to generalized Lorentzian and when $r=0$ and $q\to\infty$ the distribution $f_{(r,q)}$ reduces to the Maxwellian distribution[13]. In general, high energy tail in the profile of distribution $f_{(r,q)}$ increases as the spectral index q decreases and flat top (or shoulders) in the profile of distribution increases as spectral index r increases. Distribution functions with flat tops are often observed in space plasma [14] and these are closely resembles the distribution function given in Eq. (1) for appropriate values of *r* and *q*.

By following kinetic theory and standard text book procedure we derive the following relations for left hand and right hand circularly polarized waves, as

$$L = 1-\sum_\alpha \frac{\omega_{p\alpha}^2}{2\,\omega}\int_{-\infty}^{+\infty}\frac{v_\perp\,\hat{G}f_{r,q}\,dv^3}{k_\parallel v_\parallel-\omega+\Omega_\alpha} \quad (4)$$

$$R = 1-\sum_\alpha \frac{\omega_{p\alpha}^2}{2\,\omega}\int_{-\infty}^{+\infty}\frac{v_\perp\,\hat{G}f_{r,q}\,dv^3}{k_\parallel v_\parallel-\omega-\Omega_\alpha} \quad (5)$$

where *L* and *R* correspond to left and right hand circularly polarized waves, respectively, and the operator $\hat{G}$ is

$$\hat{G} = \left(1-\frac{k_\parallel v_\parallel}{\omega}\right)\frac{\partial}{\partial v_\perp}+\frac{k_\parallel v_\perp}{\omega}\frac{\partial}{\partial v_\parallel} \quad (6)$$

Now we consider that plasma consists of electrons and ions and using the distribution (1) in Eqs. (4) and (5), we obtained the general dispersion relation of L and R waves. Then by applying the condition for low frequency waves and considering high beta plasma, i.e. $\omega<<\Omega_i<<\Omega_e$ and $\beta_i>1$, respectively the argument of plasma dispersion functions ξ_i, becomes

$$\xi_i \simeq \frac{\Omega_i}{k_\parallel v_{thi}} \simeq \frac{\Omega_i}{v_{thi}}\frac{v_A}{\omega} \gg 1 \qquad (7)$$

We derive the dispersion relation of Alfven waves in anisotropic plasma modeled by generalized (r,q) distribution function, as

$$\omega^2(ABI_3 - AI_2) - k_\parallel{}^2 v_A{}^2 \pm \omega\frac{(ABI_5 - AI_6)(k_\parallel\psi_{i_\parallel})^2}{\Omega_i} -$$
$$\frac{\omega\, A\, \mathbb{i}\, \pi\Omega_i^2}{(k_\parallel\psi_{i_\parallel})}\left[\left(\frac{\omega\mp\Omega_i}{k_\parallel\psi_{i_\parallel}}\right)^2\left[1+\frac{\left(\frac{\omega\mp\Omega_i}{k_\parallel\psi_{i_\parallel}}\right)^{2(1+r)}}{q-1}\right]^{-q} -\right.$$
$$\left. B\left(\frac{\omega\mp\Omega_i}{k_\parallel\psi_{i_\parallel}}\right)^{2-2q-2qr} 2\hat{F}_1\right] + (ABI_5 - AI_6)D(k_\parallel\psi_{i_\parallel})^2 +$$
$$\mathbb{i}\, A\, \pi\, \Omega_i^2\, \hat{T}_i\left[\left(\frac{\omega\mp\Omega_i}{k_\parallel\psi_{i_\parallel}}\right)^3\left[1+\frac{\left(\frac{\omega\mp\Omega_i}{k_\parallel\psi_{i_\parallel}}\right)^{2(1+r)}}{q-1}\right]^{-q} -\right.$$
$$\left. B\left(\frac{\omega\mp\Omega_i}{k_\parallel\psi_{i_\parallel}}\right)^{3-2q-2qr} 2\hat{F}_1\right] = 0 \qquad (8)$$

Where $2\hat{F}_1$ is the Hypergeometric function whose argument is $\xi_i = \frac{\omega\mp\Omega_i}{k_\parallel\psi_{i\parallel}}$, (-) sign corresponds to L-wave and (+) sign corresponds to R-wave, and

$$A = \frac{3\,(q-1)^{-\frac{3}{2(r+1)}}\Gamma[q]}{4\,\Gamma\left[q-\frac{3}{2(r+1)}\right]\Gamma\left[1+\frac{3}{2(r+1)}\right]}, \qquad (9)$$

$$B = \frac{q(q-1)^q(1+r)}{q+qr-1}, \qquad (10)$$

$$D = \left(\hat{T}_i + \hat{T}_e\frac{T_{e\parallel}}{T_{i\parallel}}\right), \qquad (11)$$

$$\hat{T}_\alpha = \left(1-\frac{\psi_{\alpha\perp}^2}{\psi_{\alpha\parallel}^2}\right), \qquad (12)$$

$$I_2 = \int_{-\infty}^{+\infty} s^2\left[1+\frac{s^{2(1+r)}}{q-1}\right]^{-q} ds, \qquad (13)$$

$$I_3 = \int_{-\infty}^{+\infty} s^{2-2q-2qr}\, 2F_1\left[1+q, \frac{q-1+qr}{1+r}, \frac{q+qr+r}{1+r}, -(q-1)s^{-2(1+r)}\right] ds, \qquad (14)$$

$$I_5 = \int_{-\infty}^{+\infty} s^{4-2\,q-2\,q\,r}\, ds\; 2F1\left[1+q, \frac{q-1+qr}{1+r}, \frac{q+qr+r}{1+r}, -(q-1)s^{-2(1+r)}\right], \qquad (15)$$

$$I_6 = \int_{-\infty}^{+\infty} s^4\left[1+\frac{s^{2(1+r)}}{q-1}\right]^{-q} ds. \qquad (16)$$

In deriving the dispersion relation (8), we have used the condition $v_A^2 << c^2$ and neglect the electron terms as electrons do not take part in damping/growth due to their high frequency.

2. NUMERICAL RESULTS AND CONCLUSION

We solve the dispersion relation (8) for real and imaginary parts of frequencies and found that L-wave grows when there is temperature anisotropy; however, R-wave shows damping. In Fig.1 we plot the growth rates of L-wave for the observed temperature anisotropies $T_{i\perp}/T_{i\parallel} = 2.5$, $T_{e\parallel}/T_{i\parallel} = 0.5$ and $T_{e\perp}/T_{i\parallel} = 0.55$ from the downstream of a quasi-perpendicular shock[10]. In Fig. 1 (upper panel), we can see that as q increases for a fix value of r, the growth rate increases and approaches to Maxwellian growth but remains lower than the Maxwellian (shown in dotted line). So, the high energy tail corresponds to small values of q reduces the temperature anisotropy effect and thus the number of resonant particles. In Fig. 1 (lower panel), we can see that as the value of r increases for a fix value of q, damping rate decreases. The increase in the value of r which corresponds to the increment in the flat top in the distribution function reduces the temperature anisotropy effect and thus the number of resonant particles. Fig. 2 (upper panel) is plotted for different values of temperature ratio $T_{i\perp}/T_{i\parallel}$ when the other ratios are $T_{e\parallel}/T_{i\parallel} = 0.5$ and $T_{e\perp}/T_{i\parallel} = 0.55$.We can see that as the perpendicular ion temperature increases the growth rate increases. In Fig. 2 (lower panel), growth rate is plotted for different

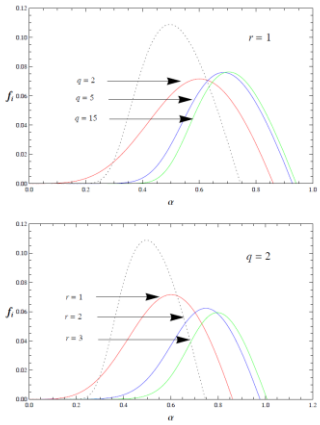

Fig. 1. Growth rates for L-wave. Dotted line represents Maxwellian growth rate

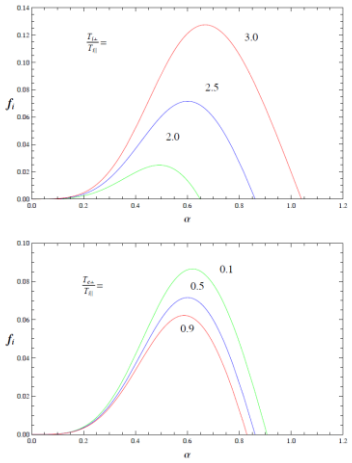

Fig. 2. Growth rates for different ratios of $T_{i\perp}/T_{i\parallel}$ when $T_{e\parallel}/T_{i\parallel} = 0.5$ and $T_{e\perp}/T_{i\parallel} = 2.5$ (upper panel) and for different ratios of $T_{e\perp}/T_{i\parallel}$ when $T_{i\perp}/T_{i\parallel} = 2.5$ and $T_{e\parallel}/T_{i\parallel} = 0.5$ (lower panel).

temperature ratio $T_{e\perp}/T_{i\parallel}$ when the other anisotropies are $T_{e\parallel}/T_{i\parallel} = 0.5$ and $T_{i\perp}/T_{i\parallel} = 2.5$. It can be noted that as the perpendicular electron temperature increases the growth rate decreases.

In this paper, growth of Left handed circularly polarized Alfven wave is studied which is introduced by proton and electron temperature anisotropies in high plasma β (in this study we have taken $\beta = 2$). It is observed that the anisotropy in the ion temperatures

increases the growth rate whereas the anisotropy in the electron to ion temperatures decreases the growth rate. Therefore, the growth in the Alfven wave is due to the ion temperature anisotropies as observed in high beta plasmas at the earth's bow shock[10,15]. Moreover, in the real situations where we use non-Maxwellian distributions, the growth rate is suppressed as compared to the Maxwellian growth rate.

Acknowledgement: This research was supported by the HEC grant no. 20-1886/R&D/10.

REFERENCES

1. A.B. Collier, A.R.W. Hughes, et al. Evidence of standing waves during a Pi_2 pulsation observed on Cluster // *Ann. Geophy.* 2006, v. 24, p. 2719-2733.
2. J. Dombeck, C. Cattell, et al. Alfven waves and poyting flux observed simultaneously by Polar and FAST in the plasma sheet boundary layer // *J. Geophys. Res*. 2005, v. 110, p. A12S90.
3. S.H. Chen, M.G. Kivelson. On ultralow frequency waves in the lobes of the earth's magnetotail // *J. Geophys. Res*. 1991, v. 96, p. 15711-15723.
4. J.R. Wygant, A. Keiling, et al. Evidence for kinetic Alfven waves and parallel electron energization at 4-6 RE altitudes in the plasma sheet boundary layer // *J. Geophys. Res.* 2002, v. 107, p. 1201-1215.
5. A. Keiling, J.R. Wygant Correlation of Alfven wave pointing flux in the plasma sheet at 4-7 RE with ionospheric electron energy flux // *J. Geophys. Res.* 2002, v. 107, p. 1132-1144.
6. A. Keiling, G.K. Parks, et al. Some properties of Alfven waves: Observations in the tail lobes and the plasma sheet boundary layer // *J. Geophys. Res.* 2005, v. 110, p. A10S11.
7. T. Takada, R. Nakamura, et al., Alfven waves in the near-PSBL lobe: Cluster observations // *Ann. Geophys*. 2006, v. 24, p. 1001-1013.
8. C.C. Chaston, C.W. Carlson, et al. Alfven waves, density cavities and electron acceleration observed from the FAST spacecraft // *Phys. Scr*. 2000, v. 84, p. 64-68.
9. R.L. Lysak. Electrrodynamic coupling of the magnetosphere and ionosphere // *Space Sci. Rev.* 1990, v. 52, p. 33-87.
10. O. Alexandrova, A. Mangeney, et al. Cluster observations of finite amplitude Alfven waves and small-scale magnetic filamennts downstream of a quasi-perpendicular shock // *J. Geophys. Res.* 2004, v. 109, p**.** A05207.
11. B.J. Anderson, S.A. Fuselier, et al. Magnetic spectral signatures in the Earth's magnetosheath and plasma depletion layer // *J. Geophys. Res.* 1994, v. 99, p. 5877-5891.
12. S.P. Garry, P.D. Convery, et al. Proton and helium cyclotron anisotropy instability thresholds in the magnetosheath // *J. Geophys. Res.* 1994, v. 99, p. 5915-5921.
13. Z. Kiran, H.A. Shah, et al. Parallel proton heating in solar wind using generalized (r,q) distribution function // *Solar Phys*. 2006, v. 236, p. 167-182.
14. C. Lacombe, F.G.E. Pantellini, et al. Mirror and Alfvenic waves observed by ISEE 1-2 during crossings of the Earth's bow shock // *Ann. Geophys*. 1992, v. 10, p. 772-784.
15. C. Lacombe, F.G.E. Pantellini, et al. Mirror and Alfvenic waves observed by ISEE 1-2 during crossings of the Earth's bow shock//*Ann. Geophys.* 1992, v. 10, p. 772-784.

Article received 25.10.12

НЕУСТОЙЧИВОСТИ АЛЬФВЕНОВСКОЙ ВОЛНЫ, ОСНОВАННЫЕ НА АНИЗОТРОПИИ ТЕМПЕРАТУРЫ С НЕМАКСВЕЛЛОВСКОЙ ФУНКЦИЕЙ РАСПРЕДЕЛЕНИЯ

M.N.S. Qureshi, Sundas Saeed, H.A. Shah

Космические наблюдения многочисленных спутников показывают, что немаксвелловские распределения часто обладают такими характеристиками, как высокие энергетические хвосты или плоские вершины (широкие плечи) в профиле функций распределения. Распределения с высокими энергетическими хвостами хорошо моделируются семейством распределений типа каппа. Однако, когда распределения содержат плоские вершины с или без высокоэнергетических частиц, тогда лучшим выбором является обобщенная (*r,q*)-функция распределения. В общем, спектральный индекс *r* соответствует плоской части распределения, а *q* соответствует высокому энергетическому хвосту в профиле функции распределения. Следуя кинетической теории, мы использовали эту функцию распределения для изучения альфвеновских волн в анизотропной плазме и обнаружили, что альфвеновская волна может расти при наличии температурной анизотропии в плазме. Условия неустойчивостей затем изучались при различных соотношениях температуры, используя параметры плазмы, которые наблюдались вниз по потоку ударной волны в CLUSTER.

НЕСТІЙКОСТІ АЛЬФВЕНОВСЬКОЇ ХВИЛІ, ЯКІ ОСНОВАНІ НА АНІЗОТРОПІЇ ТЕМПЕРАТУРИ З НЕМАКСВЕЛІВСЬКОЮ ФУНКЦІЄЮ РОЗПОДІЛУ

M.N.S. Qureshi, Sundas Saeed, H.A. Shah

Космічні спостереження чисельних супутників показують, що немаксвеллівські розподілення часто володіють такими характеристиками, як високі енергетичні хвости або плоскі вершини (широкі плечі) в профілі функцій розподілу. Розподіл з високими енергетичними хвостами добре моделюється сімейством розподілів типу каппа. Однак, коли розподіл містить плоскі вершини з або без високоенергетичних часток, тоді кращим вибором є узагальнена *(r, q)*-функція розподілу. Загалом, спектральний індекс *r* відповідає плоскій частині розподілу, а *q* – високому енергетичному хвосту в профілі функції розподілу. Відповідно до кінетичної теорії, ми використовували цю функцію розподілу для вивчення альфвенівських хвиль в анізотропній плазмі і виявили, що альфвенівська хвиля може рости при наявності температурної анізотропії в плазмі. Умови нестійкостей потім вивчалися при різних співвідношеннях температури, використовуючи параметри плазми, які спостерігалися вниз по потоку ударної хвилі в CLUSTER.